Optimized Photoelectric Performances via Composition Regulation of Precursor Solutions in $CsPbI_3$ Perovskite Solar Cells

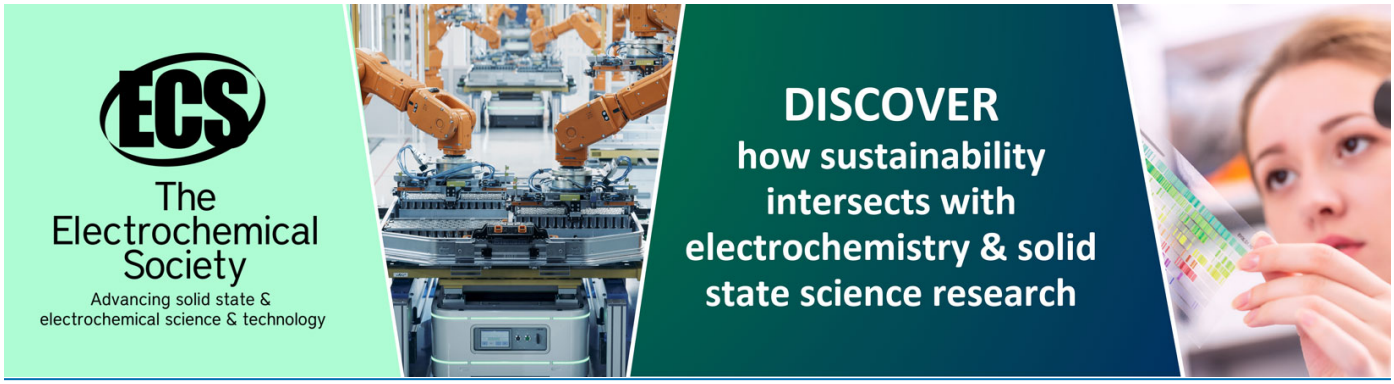

Optimized Photoelectric Performances via Composition Regulation of Precursor Solutions in $CsPbI_3$ Perovskite Solar Cells

Chuanru Dai[1a*]

[1]School of Materials Science and Engineering, School of Physics and optoelectronics engineering, Anhui University, Hefei 230601, China

[a*]b19201051@stu.ahu.edu.cn

Abstract—The composition of precursor solutions always significantly impacts the morphology and properties of perovskite films, which plays an important role in the final performance of the solar cells. Here, PbI_2 and $DMAPbI_3$ were introduced in the $CsPbI_3$ precursor solutions. The optimized composition and structure were realized by adjusting the content ratio of the two components. The optimum content ratio of PbI_2 and $DMAPbI_3$ was about 3:7, which results in a uniform film with optimized internal defects. Thus, the subsequent grain formation and growth process during the annealing process are better controlled. Finally, the obtained perovskite solar cells realized a power conversion efficiency (PCE) of 16.13%.

1. Introduction

In recent years, organic-inorganic hybrid perovskite solar cells have continuously refreshed the photoelectric conversion efficiency of the cell since its first report, and its highest efficiency has now exceeded 25%. Among them, inorganic $CsPbI_3$ perovskite solar cells have attracted the attention of many researchers due to their excellent thermal stability, high absorption coefficient, low exciton binding energy, and high carrier mobility[1-3], which are expected to be the most promising of the latest generation of commercialized thin-film solar cells. However, although $CsPbI_3$ perovskite has a suitable bandgap of 1.69~1.72 eV and excellent thermal stability, the problems of phase instability and moisture resistance are also worthy of our attention and study[4,5]. $CsPbI_3$ perovskites are prone to involuntarily transform from a black phase with optoelectronic properties to a yellow phase without photovoltaic properties at room temperature[6]. In addition, the composition of precursor solutions has always had a significant impact on the morphology and properties of thin films[7].

Nowadays, $DMAPbI_3$ and DMAI as perovskite intermediates and additives have become an effective method to prepare β-$CsPbI_3$ and γ-$CsPbI_3$ perovskites. Meng et al. found that by doping DMAI into the $CsPbI_3$ precursor solution, the non-all-inorganic perovskite $DMA_{0.15}Cs_{0.85}PbI_3$ composed of it has a more suitable bandgap of 1.67 eV, and by controlling the annealing process, it can also form Cs_4PbI_6 and $DMA_{0.15}Cs_{0.85}PbI_3$ mixed films[8]. Wang et al. pointed out that DMAI can be used as an additive to control the surface morphology and crystallization process of $CsPbI_3$ films more easily, and DMAI can be easily removed in a humid environment and high temperature[9]. Therefore, the regulation of the DMAI content in the $CsPbI_3$ perovskite precursor solution is particularly important, which has a significant impact on the subsequent morphology of the film and the performance of the solar cells.

In this work, to optimized photoelectric performances of the $CsPbI_3$ perovskite solar cells, the composition of precursor solutions was regulated. By adjusting PbI_2 and $DMAPbI_3$ in the precursor solution ($DMAI/PbI_2$ = 1~1.3 in $DMAPbI_3$), the best photoelectric performance of the solar cell device was obtained when the content ratio of PbI_2 and $DMAPbI_3$ was about 3:7.

2. Experimental Methods

2.1. Synthesis of the $DMAPbI_3$ powder

3 g PbI_2 was dissolved in 5 mL of N, N dimethylformamide. The obtained solutions were stirred and heated at 85°C for half an hour. Then, 6.5 mL hydroiodic acid was add after the PbI_2 was completely dissolved, and kept for 2-3 hours. After the yellow precipitate was completely precipitated, filtered, washed and dried, the yellow $DMAPbI_3$ powder was obtained.

2.2. Preparation of $CsPbI_3$ perovskite precursor solution

The $DMAPbI_3$ and PbI_2 powders were weighed in different proportions (decreasing proportion from 10/0 to 5/5 gradually), and the same molar ratio of cesium iodide (CsI) in were dissolved in the DMF/DMSO solvent with a ratio of 9/1 to prepare a 0.6 M $CsPbI_3$ perovskite precursor solution.
The with H-type main steel beams and steel channels, lightweight precast panels set upon the steel skeleton, shear keys connected to the main steel beams and post-pouring concrete layer.

2.3. Preparation of HTL hole transport layer solution

36 mg PTAA was dissolved in 1 mL chlorobenzene mixed with 22 μL sulfonimide (520 mg Li-TFSI in 1 mL acetonitrile), then 36 μL tert-butylpyridine (TBP) was added. Different kinds of up-conversion nanoparticles synthesized above were dissolved in the above hole transport layer solution in the amount of 0.5 mg, 1 mg, 2 mg and 5 mg/mL, respectively.

2.4. Preparation of TiO_2 electron transport layer

25×25 mm^2 FTO conductive glass was wiped, washed and dried, and then subjected to O_2 plasma treatment. The clean FTO substrate was then immersed in a 40 mM $TiCl_4$ hydrated solution and reacted at 70 °C for about 30 minutes. After the reaction, the substrate was cleaned with deionized water and ethanol. After that, the reacted substrate was heated and annealed on a hot stage at 200° C. for 30 minutes to obtain a dense n-type TiO_2 electron transport layer.

2.5. Fabrication of the $CsPbI_3$ perovskite solar cells

After the prepared TiO_2 was treated with plasma O_2, the $CsPbI_3$ perovskite film was obtained by a one-step spin coating method, and the film was annealed at 200 °C on a hot stage after spin coating for 5 to 10 minutes. Then the hole transport layer PTAA was spin-coated and annealed at 75 ° C for 5 minutes. Finally, the 80 nm thick Au electrode was heated and evaporated onto the PTAA layer to obtain a complete $CsPbI_3$ perovskite solar cells.

3. Result and discussion

3.1. Characterizations

To optimize the composition and structure of the $CsPbI_3$ precursor solutions, different ratios of $DMAPbI_3$ and PbI_2 powders were used to prepare the obtained films. First, the control variable method was conducted to prepare the precursor solutions with different content ratios of $DMAPbI_3$ and PbI_2. Then, the $CsPbI_3$ perovskite films with different content ratios were obtained after spin-coating and annealing in a glove box by the one-step spin-coating method. Wang's group has confirmed that the DMAI organic matter contained in $DMAPbI_3$ is only used as an additive to improve the crystallization mode of the film, which itself can be removed by heating. This method is similar to an ion-exchange method to remove organic components in $CsPbI_3$. Pang et al. used cation exchange to repair the film,

and the methylamine group (MAX) in the $CsPbI_3$ perovskite film was removed by MA gas repair and heating. They found that higher quality γ-$CsPbI_3$ films could be obtained by controlling the content of MAX and MA gases and using cation exchange, and the films with optimized concentrations had better surface interfaces, lower defect states and better stability[10]. This method helps us to obtain higher quality $CsPbI_3$ perovskite films. As shown in Fig. 1, the SEM images of the obtained films were exhibited. Clearly, when the proportion of $DMAPbI_3$ is high, there are a few holes and inhomogeneous composition on the surface of the $CsPbI_3$ film. With the increase of PbI_2 ratio, the grains in the films are more plump and more regular, without holes and obvious white areas were observed at the grain boundaries. However, when the ratio of $DMAPbI_3$ and PbI_2 reaches 1:1, as shown in Figure 1c, the particle volume of the crystal grains is significantly reduced, and the film becomes discontinuous, with more grooves on the surface, which has a greater impact on the optoelectronic properties of the device. Researchers from Anita's group reported that when the $CsPbI_3$ film was prepared by ion exchange, the formation of the film was controlled by the template of $MAPbI_3$. When the ion exchange occurred, the resulting film was pinhole-free and smooth[11]. Therefore, the amount of DMA^+ cations in the precursor solution similarly affects and manipulates the formation quality of the films in our work. After optimizing a series of ratios, we found that when the ratio of DMA-PbI_3 and PbI_2 was about 7:3, the topographical quality of the film was the best.

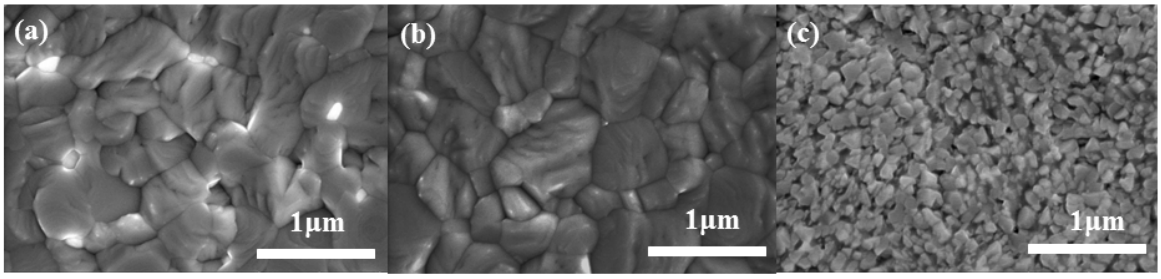

Fig.1 SEM images of $CsPbI_3$ films prepared by different proportions of $DMAPbI_3/PbI_2$: (a) $DMAPbI_3/PbI_2$ =10:0; (b) $DMAPbI_3/PbI_2$ =7:3; (c) $DMAPbI_3/PbI_2$ =1:1.

In order to explore the effect of different content ratios of $DMAPbI_3$ and PbI_2 on the structure of the formed $CsPbI_3$ films, XRD diffraction was conducted. As shown in Figure 2a, through the XRD diffraction pattern, we can find that the film shows the characteristic peaks of $CsPbI_3$ perovskite at 14.4° and 28.8°, which correspond to the (110) and (220) crystal planes, respectively. When the ratio of $DMAPbI_3$ to PbI_2 is 7:3, the intensity of the characteristic peaks of the $CsPbI_3$ film is obviously enhanced without shifting, and the peak intensities of other non-perovskite phases are relatively suppressed. When the ratio of $DMAPbI_3$ continuously increased to the same molar ratio of PbI_2, the intensities of the XRD diffraction peaks of the thin films are obviously weakened, and the peak intensity of the non-perovskite phase is also enhanced. The intensity of the XRD diffraction peaks corresponds to the surface topography of the thin film in Figure 1. Wang et al. speculated that the amount of DMAI would affect the control of the crystallization kinetics of $CsPbI_3$. During the annealing process, with the sublimation of DMAI, Cs cations will enter the crystal lattice, and a relatively small amount of DMAI will accelerate the film crystallization process[9].

3.2. Photoelectric performance

In order to explore the effect of different content ratios of $DMAPbI_3$ and PbI_2 on the optical properties of the obtained $CsPbI_3$ films, UV-vis absorption and photoluminescence characterization were conducted. As shown in Figure 2b, when the ratio of $DMAPbI_3$ and PbI_2 reaches 7:3, the $CsPbI_3$ film has the highest UV-vis absorption intensity, and the absorption spectrum exceeds 700 nm. When the ratio of PbI_2 is further increased, the absorption intensity of the film is reduced. The reason is that when the amount of DMAI is small, it is difficult for the film to form β-$CsPbI_3$ or γ-$CsPbI_3$ at a

temperature of 200 °C, and the quality of the film is also poor, thus the grains become smaller and the pores increase.

In order to explore the effect of different ratios of $DMAPbI_3$ and PbI_2 on the defects and non-radiative recombination centers at the surface and interface of $CsPbI_3$ films, we tested the photoluminescence spectra and fluorescence lifetimes of different kinds of films. As shown in Figure 2c, it can be seen that the $CsPbI_3$ film, which was prepared by spin coating on the same substrate, the intensity of the fluorescence emission peak is the highest when the ratio of $DMAPbI_3$ and PbI_2 is 7:3. After normalization, the slight redshift is almost negligible. At the same time, the steady-state fluorescence lifetime test was performed on the film again. The graph and table drawn by the experimental data are shown in Figure 2d and Table 1. It can be calculated that, the fluorescence decay lifetime of the film is the longest when the proportion of $DMAPbI_3$ reaches 70%, which indicates that the film has fewer grain defects and fewer non-radiative recombination centers. This is beneficial to the separation and transport of carriers. Researchers such as Sherker pointed out that the defects at the interface and grain boundary will affect the exciton lifetime to a certain extent, and ultimately affect the optoelectronic properties of perovskite cells. When the film is relatively dense, the trap defects at the grain boundaries have a certain influence on the performance of the film. On the other hand, when the film is in a non-dense state, the performance of the battery device is greatly affected by the defects on the surface of the film. Moreover, the trap defects at the grain boundary and the trap recombination of the interface state have a greater impact on the photocurrent and voltage of the device[12, 13]. Therefore, combined with the scanning electron microscope image of the surface morphology in Figure 1, the dense grain morphology of the film surface has fewer trap defects, while the increase of grain boundaries. Meanwhile, the unevenness of the film surface will undoubtedly increase the probability of trap states on the surface of the film. In the follow-up work, we will conduct further research and experiments on how to reduce the defects at the surface and grain boundaries.

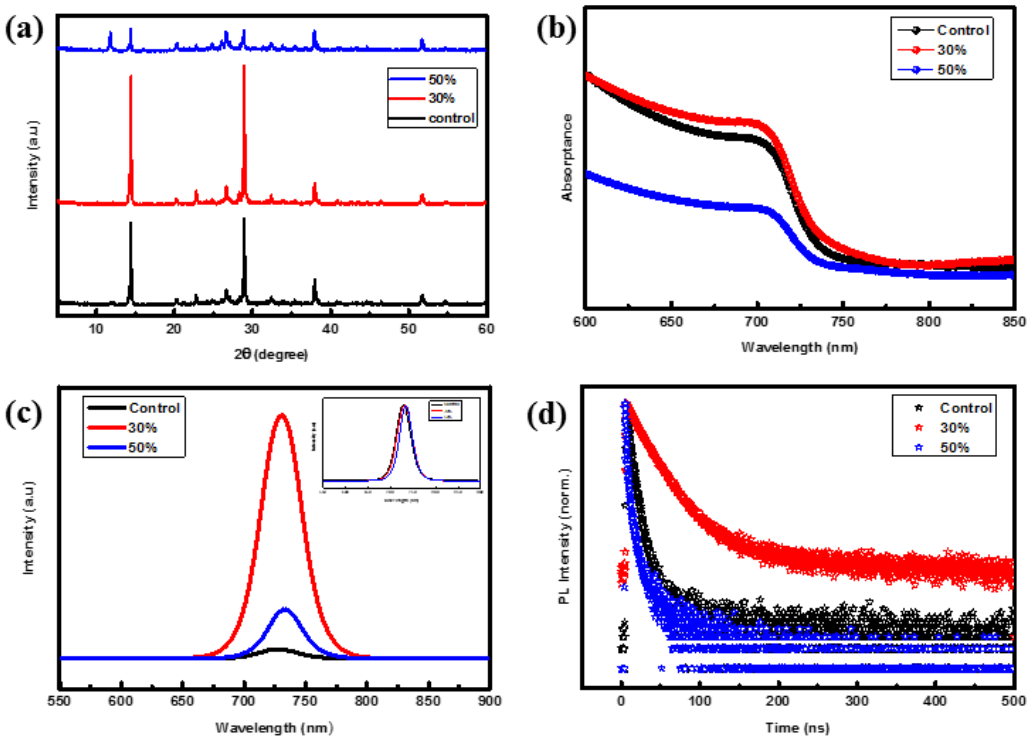

Fig.2 Comparison of characteristics of $CsPbI_3$ films prepared by different proportions of $DMAPbI_3/PbI_2$: (a) XRD patterns, (b) Absorption spectra, (c) PL spectra and (d) TRPL spectra.

Tab.1 Parameters of the TRPL spectra of $CsPbI_3$ films prepared by different proportions of $DMAPbI_3/PbI_2$: (extracted from Figure 2d).

Device	τ_{ave} (ns)	τ_1 (ns)	τ_2 (ns)	A_1 (ns)	A_2 (ns)
control	5.59	13.14	4.33	5.23	94.77
30%	20.68	65.28	9.50	3.52	96.48
50%	3.08	7.71	1.19	5.94	94.06

To test the effect of different ratios of $DMAPbI_3$ and PbI_2 on the photoelectric conversion efficiency of $CsPbI_3$ perovskite solar cells, J-V tests of the photoelectric properties of the devices were conducted. The curve parameters of all J-V tests such as open circuit voltage (V_{oc}), short circuit current (J_{sc}), impact factor (FF) and photoelectric conversion efficiency are shown in Figure 3a and Table 2. The reference $CsPbI_3$ perovskite solar cell has an efficiency of 15.01%, corresponding to a J_{sc} of 19.42 mA/cm^2, a V_{oc} of 1.04 V and a FF of 73.93%. When the proportion of PbI_2 is reduced to 30%, the overall photoelectric conversion efficiency of the $CsPbI_3$ perovskite solar cell is improved, and its highest photoelectric conversion efficiency can be as high as 16.13%. At the same time, other photoelectric parameters are also improved accordingly. The main reason is that the device film obtained by this ratio has the highest quality and fewer defects, resulting in strong absorption of visible light. Besides, the corresponding non-radiative recombination is also significantly reduced, thus enhancing the diffusion and transport of carriers. However, when the ratio of the two reaches 1:1, the photoelectric efficiency of the device is significantly reduced. It is mainly caused by the increase of trap states at the surface and grain boundaries of the thin film of the perovskite light-absorbing layer. In order to ensure the reliability of the short-circuit current, we conducted a constant current test under the constant voltage of the maximum power point with stable illumination, and found that the photocurrent current did not decrease significantly, indicating that the high reliability of our short-circuit current.

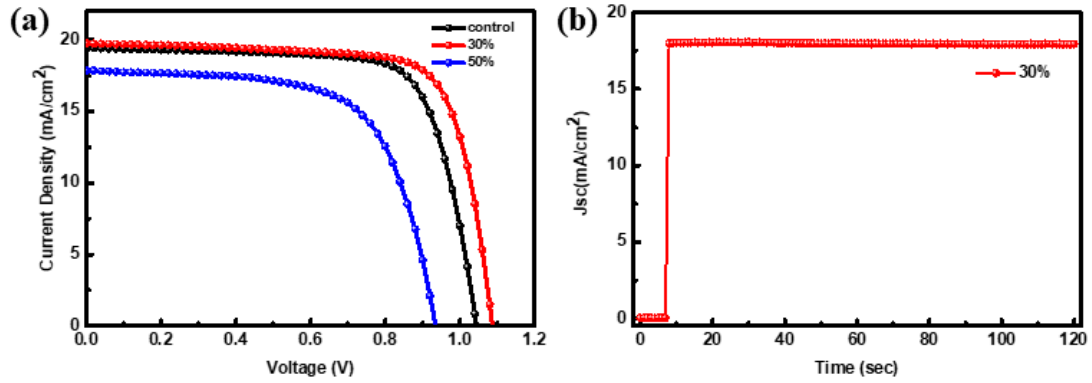

Fig.3 (a) Comparison of the J-V characteristics of $CsPbI_3$ PSCs prepared by different proportions of $DMAPbI_3/PbI_2$, (b) J_{sc} measured as a function of time for the cells biased at V_{max}.

Tab.2 Comparison of the J-V characteristics of $CsPbI_3$ PSCs prepared by different proportions of $DMAPbI_3/PbI_2$ (extracted from Figure 3a).

Device	J_{sc} (mA/cm^2)	V_{oc} (V)	FF (%)	PCE (%)
control	19.42	1.04	73.93	15.01
30%	19.76	1.08	75.12	16.13
50%	17.86	0.93	65.65	10.94

4. Conclusion

In this work, the ratio of $DMAPbI_3$ and PbI_2 was adjusted to study how the composition of the $CsPbI_3$ precursor solution affects the performance of the perovskite solar cell devices. The main conclusions can be summarized as follows: (1) the amount of DMA^+ cations in the precursor solution seriously affects the formation quality of the films; (2) with the optimized ratio, the film is more uniform, and the internal defects are improved to a certain extent; (3) the grain formation and growth process during the annealing process can also be better controlled; (4) the defects at the interface and grain boundary will affect the exciton lifetime, which ultimately affects the optoelectronic properties of perovskite cells. In terms of the future work, the composition of the precursor solutions should be optimized to enhance the photoelectric properties of the $CsPbI_3$ perovskite solar cell devices.

Acknowledgments

This work was financially supported by the Key Projects of Natural Science Research in Universities of Anhui Province (KJ2020A0018).

References

[1] Ho-Baillie A, Zhang M, Lau C F J, et al. Untapped Potentials of Inorganic Metal Halide Perovskite Solar Cells [J]. Joule, 2019, 3(4): 938-955.
[2] Faheem M B, Khan B, Feng C, et al. All-Inorganic Perovskite Solar Cells: Energetics, Key Challeng-es, and Strategies toward Commercialization [J]. ACS Energy Letters, 2020, 5(1): 290-320.
[3] Xiang W, Tress W. Review on Recent Progress of All-Inorganic Metal Halide Perovskites and Solar Cells [J]. Advanced Materials, 2019, 31(44): 1902851.
[4] Chen H, Xiang S, Li W, et al. Inorganic Perovskite Solar Cells: A Rapidly Growing Field [J]. Solar RRL, 2018, 2(2): 1700188.
[5] Ye Q F, Zhao Y, Mu S Q, et al. Stabilizing the Black Phase of Cesium Lead Halide Inorganic Perovskite for Efficient Solar Cells [J]. Science China-Chemistry, 2019, 62(7): 810-821.
[6] Voznyy O. Black and Stable: A Path to All-Inorganic Halide Perovskite Solar Cells [J]. Joule, 2018, 2(7): 1215-1216.
[7] Zhu W, Zhang Q, Chen D, et al. Intermolecular Exchange Boosts Efficiency of Air-Stable, Car-bon-Based All-Inorganic Planar $CsPbIBr_2$ Perov-skite Solar Cells to Over 9% [J]. Advanced Ener-gy Materials, 2018, 8(30): 1802080.
[8] Meng H, Shao Z, Wang L, et al. Chemical Compo-sition and Phase Evolution in DMAI-Derived In-organic Perovskite Solar Cells [J]. ACS Energy Letters, 2019, 263-270.
[9] Zhao Y, Wang Y, Liu X, et al. The Role of Dime-thylammonium Iodine in $CsPbI_3$ Perovskite Fab-rication: Additive or Dopant? [J]. Angewandte Chemie, 2019, 131(46): 16844-16849.
[10] Shao Z, Wang Z, Li Z, et al. A Scalable Methyla-mine Gas Healing Strategy for High-Efficiency Inorganic Perovskite Solar Cells [J]. Angewandte Chemie International Edition, 2019, 58(17): 5587-5591.
[11] Lau C F J, Wang Z, Sakai N, et al. Fabrication of Efficient and Stable $CsPbI_3$ Perovskite Solar Cells through Cation Exchange Process [J]. Advanced Energy Materials, 2019, 0(0): 1901685.
[12] Sherkar T S, Momblona C, Gil-Escrig L, et al. Re-combination in Perovskite Solar Cells: Signifi-cance of Grain Boundaries, Interface Traps, and Defect Ions [J]. ACS Energy Letters, 2017, 2(5): 1214-1222.
[13] Zhang J, Wang Z, Mishra A, et al. Intermediate Phase Enhances Inorganic Perovskite and Metal Oxide Interface for Efficient Photovoltaics [J]. Joule, 2019, 4(1): 222-234.